Title	Evaluating the surface chemistry of black phosphorus during ambient degradation
Authors	van Druenen, Maart;Davitt, Fionán;Collins, Timothy W.;Glynn, Colm;O'Dwyer, Colm;Holmes, Justin D.;Collins, Gillian
Publication date	2019-01-14
Original Citation	van Druenen, M., Davitt, F., Collins, T., Glynn, C., O'Dwyer, C., Holmes, J. D. and Collins, G. (2019) 'Evaluating the Surface Chemistry of Black Phosphorus during Ambient Degradation', Langmuir, 35(6), pp. 2172-2178. doi:10.1021/acs.langmuir.8b04190
Type of publication	Article (peer-reviewed)
Link to publisher's version	https://pubs.acs.org/doi/10.1021/acs.langmuir.8b04190 - 10.1021/acs.langmuir.8b04190
Rights	© 2019, American Chemical Society. This document is the Accepted Manuscript version of a Published Work that appeared in final form in Langmuir, © American Chemical Society, after peer review and technical editing by the publisher. To access the final edited and published work see https://pubs.acs.org/doi/abs/10.1021/acs.langmuir.8b04190
Download date	2025-06-01 01:46:45
Item downloaded from	https://hdl.handle.net/10468/7340

LANGMUIR

Evaluating the Surface Chemistry of Black Phosphorus during Ambient Degradation

Maart van Druenen, Fionán Davitt, Timothy Collins, Colm Glynn, Colm O'Dwyer, Justin D. Holmes, and Gillian Collins

Just Accepted

ACS Publications

Evaluating the Surface Chemistry of Black Phosphorus during Ambient Degradation

Maart van Druenen[1, 2], Fionán Davitt[1, 2], Timothy Collins[1], Colm Glynn[1], Colm O'Dwyer[1],

Justin D. Holmes[1, 2] and Gillian Collins[1, 2,*]

[1]*School of Chemistry, ERI & Tyndall National Institute, University College Cork, Cork, T12 YN60, Ireland.*

[2]*AMBER@CRANN, Trinity College Dublin, Dublin 2, Ireland.*

*To whom correspondence should be addressed: Tel: +353 (0)21 4905143; E-mail:

g.collins@ucc.ie

Keywords: Black phosphorus, 2D materials, phosphorene, ambient stability, degradation, oxidation, x-ray photoelectron spectroscopy, Fourier transform infrared spectroscopy

Abstract

Black Phosphorus (BP) is emerging as a promising candidate for electronic, optical and energy storage applications, however its poor ambient stability remains a critical challenge. Evaluation of few-layer liquid exfoliated BP during ambient exposure using x-ray photoelectron spectroscopy (XPS) and attenuated total reflectance Fourier transform infrared spectroscopy (ATR-FTIR) allows its surface chemistry to be investigated. Oxidation of liquid exfoliated few-layer BP initially occurs through non-bridging oxide species, which convert to

bridging oxide species after ambient exposure. We demonstrate the instability of these bridging oxide species, which undergo hydrolysis to form volatile phosphorus oxides and evaporate from the BP surface. FTIR spectroscopy, scanning transmission electron microscopy and atomic force microscopy were used to confirm the formation of liquid oxides through a continuous oxidation cycle that results in the decomposition of BP. Furthermore, we show that the instability of few-layer BP originates from the formation of bridging oxide species.

Introduction

Black phosphorus (BP) is a crystalline layered material consisting of phosphorene layers stacked together by van der Waals interactions. Since the isolation of two dimensional phosphorene from bulk BP, it has gained significant interest due to its high carrier mobility and direct bandgap that is tunable with layer thickness.[1–4] The ambient instability of BP remains the limiting factor of its processing in many applications.[5–8] Few-layer BP displays an increased reactivity compared to other 2D materials due to its puckered honeycomb lattice structure with lone pairs on the surface which react under ambient conditions.[9,10] Degradation occurs within days for solvent exfoliated[4] and hours for mechanically exfoliated[3,4,11] BP. While many reports have observed the formation of liquid droplets on the BP surface using atomic force microscopy (AFM) and transmission electron microscopy (TEM) analysis when exposed to ambient conditions[11,12], quantification of the oxide formation and subsequent degradation can be difficult using these techniques. Recently, Abellán *et. al.*[13] developed a reliable method to characterize oxidation using AFM and Scanning Raman Microscopy by showing how thickness and crystal orientation affect the A^1_g/A^2_g ratio which is used to monitor the degree of oxidation.[13] However, assignment of the degradation products is often conflicting due to the lack of chemical identification and therefore liquid formation has been ascribed to adsorbed

water[11,14] or various phosphorus oxides (P_xO_y).[12,15] XPS analysis is a surface sensitive technique that can provide a more accurate description of BP surface degradation products.[16–19] The oxide shoulder of the P 2p core level can consist of several phosphorus oxides occurring in the 132-136 eV binding energy (BE) range.[17] Theoretical studies have predicted various oxide structures that form on the BP surface which can be observed using XPS analysis.[16]

Literature reports have displayed conflicting results with respect to the effect of water on the degradation of BP. Initially, reports proposed a hydrophilic BP surface and the droplets present on the surface after exposure were identified as ambient water, which grew in size when exposed to increased humidity levels.[11,14] Theoretical studies[20] suggested that water does not interact with the pristine BP surface but the interaction becomes favorable once the surface is oxidized. The droplets that appear as a result of degradation have also been identified as phosphoric acid[19,21] which is consistent with the decrease in pH observed during oxidation of BP in solution.[22] Huang *et. al.*[24] first reported the hydrophobic nature of the pristine BP surface and demonstrated that as the surface oxidizes, it becomes more hydrophilic which increases the ease with which water absorbs and reacts with the surface. The contribution of different oxidants to BP oxidation has been widely debated in the literature. Favron e*t. al.*[21] reported the presence of a combination of water, oxygen and light are needed for BP oxidation. Experimental studies[23,24] show that aqueous solutions of BP are stable, which are supported by theoretical studies that suggest water does not interact with pristine BP.[25] However, once the BP surface has been oxidized, oxygen defects facilitate reaction with water inducing further oxidation.[10,23,25] Xu *et. al.*[26] demonstrated the synergetic effect of oxygen and water co-adsorption on BP surface degradation using theoretical calculations. Many previous reports have investigated the interaction of water and oxygen with mechanically exfoliated BP in both light and dark environments, with a combination of water, oxygen and light resulting in a faster

3

degradation rate.[12,15,13] Favron *et. al.*[21] revealed the degradation of mechanically exfoliated few-layer BP occurs through photo-oxidation and the degradation rate is dependent on flake thickness. The oxidation of mechanically exfoliated BP in a dark environment was studied by Hu *et. al.*[15], where adsorption of water initiates degradation by enhancing the affinity of oxygen adsorption. Abellán *et. al.*[13] reported the lifetime of few-layer BP can be extended to 30 days by storing samples in dark conditions which also indicates light plays a significant role in the oxidation of BP. Kuntz *et. al.*[17] investigated the surface chemistry of liquid exfoliated BP using a combination of XPS and theoretical studies, observing a uniform oxide layer produced at the basal plane when exposed to oxygen, while water oxidizes edge and defect sites which are introduced after initial exposure to oxygen. Additionally, loss of edges and in some cases full layers occurred after ambient exposure, an effect also seen by Edmonds *et. al.*[18] through a reduction in flake thickness after XPS analysis, which was attributed to the removal of volatile phosphorus oxides by the high-vacuum of the instrument. Removal of BP layers in ambient conditions has also been reported by Island *et. al.*[14] and Castellanos-Gomez *et. al.* [11] who proposed a layer-by-layer etching process occurs during ambient exposure. Degradation of BP has been subject to theoretical studies which also reveal some contradictory conclusions. DFT studies by Ziletti *et. al.*[10] show that the formation of interstitial oxygen bridges cause deformation which can result in the crystal structure of BP breaking apart. In contrast, other theoretical studies have suggested the formation of P-O-P bonds can stabilize BP by forming a native oxide.[27]

In this article, we focus on the chemical changes occurring during the degradation of liquid exfoliated few-layer BP using combined attenuated total reflectance Fourier transform infrared (ATR-FTIR) spectroscopy and X-ray photoelectron spectroscopy (XPS). We demonstrate a continuous oxidation process takes place, leading to removal of the BP surface. The high reactivity of P-O-P species is confirmed, which are susceptible to hydrolysis[28] and contribute

4

to the oxidation of the BP lattice in correlation with theoretical studies by *Ziletti et. al.*[10] Additionally, the oxidation of few-layer and multilayered bulk BP are investigated to evaluate the differences in their degradation chemistries and the higher reactivity of few-layer BP. Insight into the few-layer BP surface chemistry as it interacts with ambient atmosphere will facilitate the discovery of new stabilization routes.

Experimental Section

BP Exfoliation

BP was purchased from Smart Elements (purity 99.998 %) and anhydrous N-metyl-2-pyrrolidone (NMP) and acetonitrile (ACN) were purchased from Sigma-Aldrich. BP was stored in a glovebox prior to use. Exfoliation of BP in degassed and Ar saturated NMP using a bath sonicator (Branson 1800) for 20 h with cooling (< 25 ºC) was carried out under inert conditions using a Schlenk line. The exfoliated solution was left to settle overnight. An exfoliated BP sample was obtained by centrifuging at 2000 rpm for 30 min and discarding the sediment, followed by centrifugation at 14500 rpm for 1 h. The discarded sediment was used as a multilayered bulk sample. The exfoliated sample was purified using $3 \times$ ACN washes and was subsequently dropcast on Si wafers or Ti substrates for XPS analysis. Samples were exposed to light, ~60 % humidity and temperature was kept constant at 19 °C during degradation.

Characterization

X-Ray photoelectron spectroscopy (XPS) analysis was carried out on an Oxford Applied Research Escabase XPS system with a base pressure of 5 x 10^{-10} mbar and a nonmonochromated Al Kα X-Ray source at 200 W. Survey spectra were recorded at 0-1000 eV at a step size of 0.7 eV, a dwell time of 0.3 s and a pass energy of 100 eV. Core levels scans were acquired at a step size of 0.1 eV, a dwell time of 0.1 s and a pass energy of 20 eV.

5

CasaXPS software was used for spectra processing with peaks corrected to a Shirley background and fitted to Voigt profiles. Charge correction was applied to the C 1s peak at 285 eV. Attenuated total reflectance infrared (ATR-IR) spectra were acquired using a Nicolet 6700 Infrared Spectrometer, with a liquid cooled MgCdTe detector and Smart iTR accessory. Spectra were collected under ambient conditions at a resolution of 2 cm^{-1} and averaged over 300 scans. Raman scattering spectra were collected using a QE65PRO OceanOptics spectrometer with a 50 μm width slit and a microscope with a 40 × objective to focus on the surface of substrates. A Laser Quantum GEM DPSS 532 nm laser was used for excitation. AFM analysis was performed on a Park XE-100 AFM system in non-contact mode with SSS-NCHR enhanced resolution tips, the XY and Z resolution are ~ 2 nm and 0.05 nm. Scanning transmission electron microscopy (STEM) analysis was acquired on an FEI Helios NanoLab 600i scanning electron microscope operating at 20 kV. Transmission electron microscopy (TEM) analysis was acquired on a Jeol 2100 at an operating accelerating voltage of 200 kV.

Results and Discussion

Liquid exfoliation in NMP was used to produce few-layer BP using bath sonication for 20 h. Figures 1(a) and (b) and Figure S1 (see Supporting Information) display TEM and STEM images of exfoliated BP flakes, which maintain their crystallinity. Retention of the crystal structure was confirmed by TEM, as *d*-spacings of 0.44 and 0.33 nm were observed corresponding to (100) and (010) planes.[29] Minimal damage was caused by the exfoliation process, as demonstrated by Raman analysis displayed in Figure 1(c). Peaks at 367, 444 and 472 cm^{-1} correspond to the A^1_g, B^2_g and A^2_g BP phonon modes in agreement with literature reports.[4,11] Figure 1(d) displays a photoluminescence spectrum from exfoliated BP, with peaks occurring at 600 and 900 nm corresponding to mono- and bilayer BP[4], suggesting exfoliation

6

down to monolayer thicknesses. AFM analysis in Figure S2 also displays the presence of flakes with ~1 and ~2 nm height, corresponding to mono- and bilayer BP flakes.[1] Furthermore, the distribution of flake heights confirms ~80 % of flakes are below 10 nm in thickness.
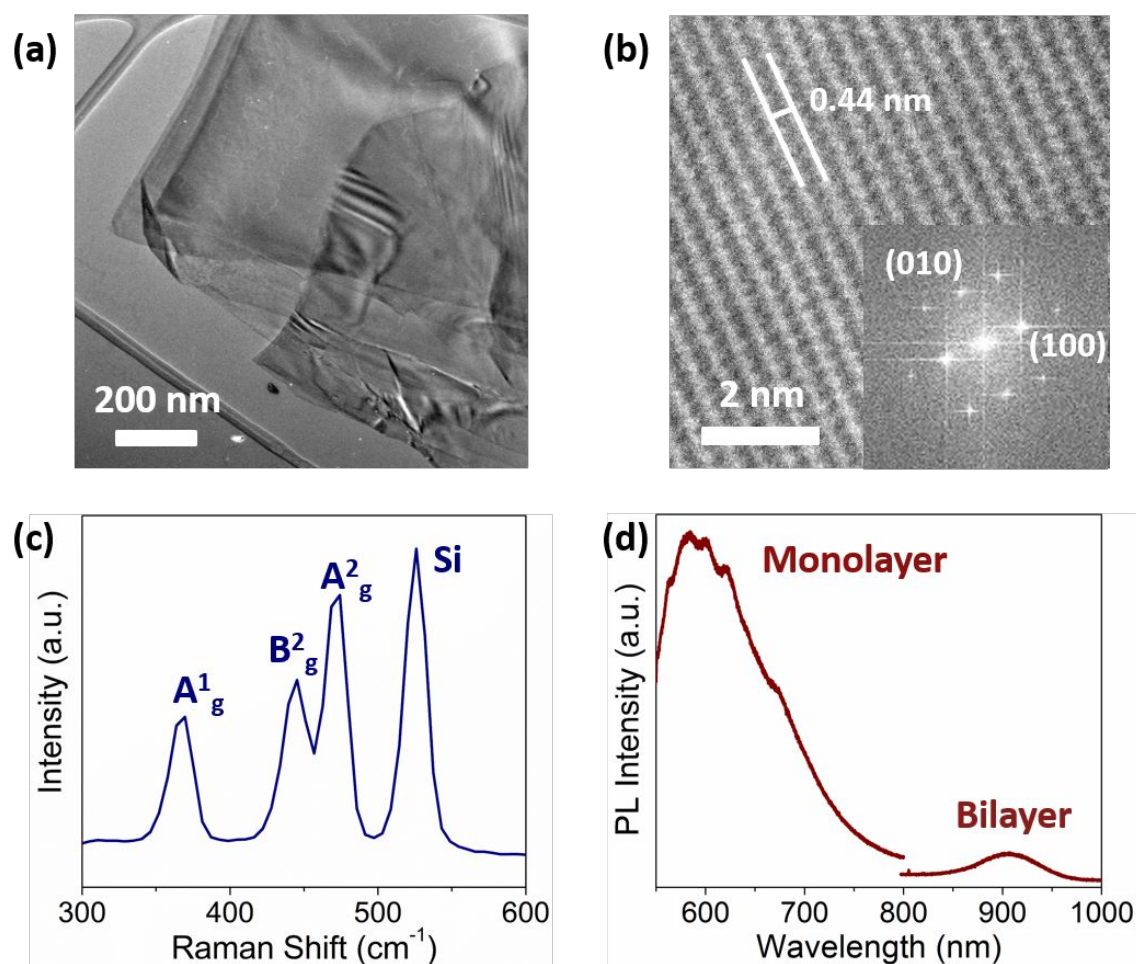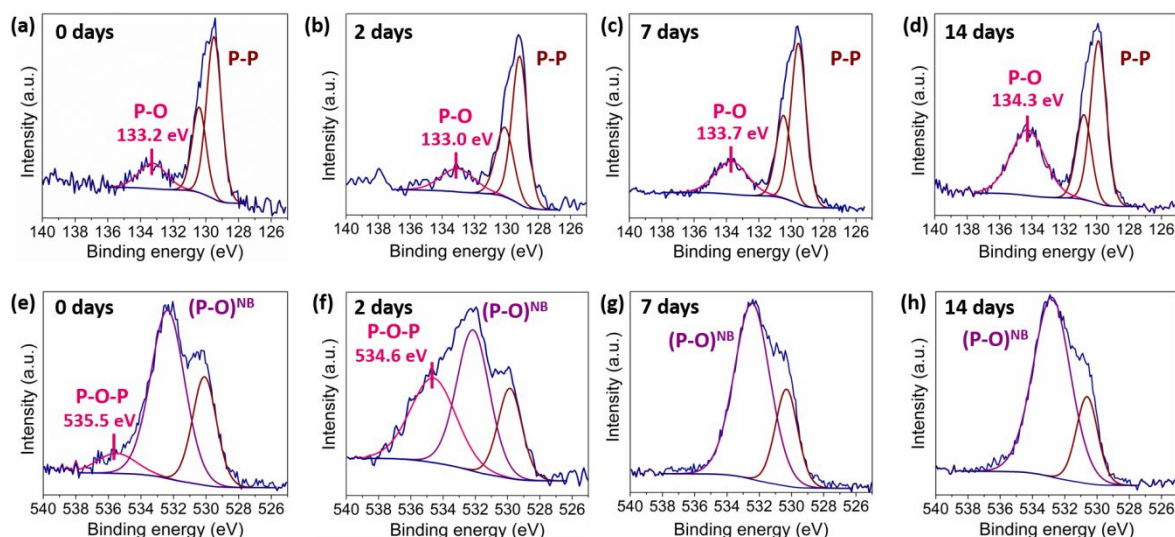

Figure 1: Liquid exfoliated few-layer BP was analyzed using (a) TEM and (b) a high-resolution image displays d-spacing with the inset showing FFT of (010) and (100) planes. (c) Raman and (d) PL spectra of liquid exfoliated BP.

Evaluation of the P 2p and O 1s core levels and FTIR spectra after aging in ambient conditions can allow the oxidation products resulting from degradation to be determined. Figure 2(a) displays the P 2p peak for freshly exfoliated BP with the elemental P peak located at a BE of 129.6 eV and an oxide shoulder at 133.2 eV, comprising 20 % of the P 2p peak, which is a typical oxide content for liquid exfoliated BP.[4] The relatively broad oxide peak ranges from 131-136 eV and consists of different phosphorus oxides species, which cannot be readily deconvoluted.[17] Removal of dissolved oxygen is a critical step in reducing oxidation during the exfoliation stage. BP oxidation during exfoliation can be reduced to 13 % (see Figure S3 in Supporting Information) by solvent degassing using several freeze-pump-thaw cycles, followed by purging the solvent with Ar. Figures 2(a)-(d) show the evolution of the P 2p core levels of BP during ambient exposure over 2 weeks. Initially the oxide shoulder at 133.2 eV consists of 16.4 % of the P 2p core level. After 2 days there was a slight increase (2 %) to 18.3 % in the P-O peak intensity but a downward peak shift of 0.2 eV was observed, suggesting an increase of species in a lower P oxidation state. A further minor increase in the oxide peak intensity of 4 % to 22.4 % was observed after 7 days and the P-O peak shifted upwards to 133.7 eV. After 2 weeks of ambient exposure a further increase in the peak intensity of 15 % occurred, with the oxide shoulder now consisting of 37 % of the total P 2p core level. The P-O shoulder further shifted upwards from 133.7 eV to 134.3 eV.

The O 1s core level can provide additional insight into the chemical changes occurring at the BP surface, as the peak can be deconvoluted into different phosphorus oxide components. Figures 2 (e)-(h) highlight the O 1s spectra of BP over 2 weeks of ambient exposure, showing three phosphorus oxide environments. The O 1s component at 530 eV can be assigned to $P^{<5+}$ species[19], however some contribution of the TiO_2 substrate which also occurs at this BE may be present. The component at ~532 eV can be assigned to non-bridging P-O environments[19]

$((P-O)^{NB})$, mainly P-O-H and P=O groups. The bridging oxide component (P-O-P) can be observed at ~535 eV.[19] The O 1s core level of freshly exfoliated BP displayed in Figure 2(e) shows the presence of 9 % bridging and 63 % non-bridging oxide species of the total O 1s core level. After 2 days of ambient exposure, the intensity of the bridging oxide species increases significantly to 36 % at the expense of non-bridging species which decrease to 42 %, as shown in Figure 2(f). The O 1s spectra indicate a conversion of non-bridging to bridging oxide species which also correlates with the negative peak shift in the P-O peak intensity observed in the P 2p core level (Figure 2(b)). A reduction in the P oxidation state would be associated with the conversion of non-bridging to bridging oxide species. After 7 days of ambient exposure the P-O-P component in the O 1s core level disappeared with only non-bridging P-O species remaining, as shown in Figure 2(g). Oxidation of BP could give rise to the production of volatile oxides as seen by Kuntz *et. al.*[17] and Edmonds *et. al.*[18]. The formation of liquid oxidation products such as phosphoric acid have been shown to evaporate under the high-vacuum environment within the XPS analysis chamber.[16,18] After 2 weeks of ambient exposure, the peak intensity of the non-bridging oxide species increases as shown in Figure 2(h), which further correlates with the increase in the P 2p oxide shoulder.

The variation in the P 2p and O 1s core levels after 2 days of ambient exposure indicate the initial formation of a surface oxide consisting mostly of non-bridging P-O species, which convert to bridging oxide species after further ambient exposure, as displayed in Figure 3. Theoretical studies[10] reported the exothermic chemisorption of oxygen both as a dangling and bridging configuration. The bridging oxide configuration, where oxygen replaces a phosphorus atom in the lattice, induces deformation that reduces the stability of the BP lattice. The instability of P-O-P species reported by Ziletti *et. al.*[10] correlates to a +4 oxidation state which is highly unfavorable, in agreement with our XPS analysis.

Figure 2: (a)-(d) P 2p and (e)-(h) O 1s core-level spectra of few-layer liquid exfoliated BP with different periods of ambient exposure.
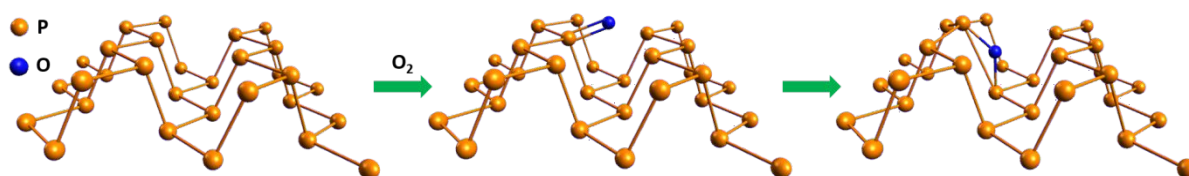
Figure 3: The oxidation of few-layer BP is initiated by the formation of non-bridging oxide species. Further oxidation occurs through the formation of bridging oxide species which are highly unstable.

The formation of a stable oxide, in the form of phosphorus pentoxide, has been reported on bulk BP surfaces.[18] However, mono- and few-layer BP can display different oxidation mechanisms to bulk BP due to an increase in surface area and a larger contribution of edge effects. The characteristic BE for phosphorus pentoxide is 135 eV[30] which cannot be readily deconvoluted from the oxide shoulder in BP. Additionally, liquid oxidation products such as

phosphoric acid occur at a similar BE of 134.5 eV[18] and are difficult to analyze using XPS analysis due to their volatility under vacuum conditions. ATR-FTIR analysis was used to distinguish between the formation of phosphorus pentoxide and phosphoric acid. The appearance of a peak associated with P-O-P species in the 850-900 cm^{-1} range[31–33] can allow identification of bridging oxide species while the formation of phosphoric acid can be confirmed by the presence of PO_3 absorptions.[33] Figure 4 and Table 1 display the ATR-FTIR analysis of liquid exfoliated few-layer BP over a 1 week period of ambient exposure. ATR-FTIR analysis of freshly exfoliated BP displays a large absorption peak at 1650 cm^{-1} which can be attributed to O=P-OH species[34] as well as two stretches at 1400 and 1300 cm^{-1} which can be assigned to P=O groups.[34,35] An asymmetric PO_2 stretch was observed at 1260 cm^{-1} while symmetric and asymmetric PO_3 stretches occurred at 1115 and 985 cm^{-1}.[33] The presence of absorptions associated with P=O during the initial exposure period indicates a dissociative reaction of oxygen with the BP surface, in correlation with DFT calculations as reported by Huang *et. al.*[23].

Following 1 day of ambient exposure, the ATR-FTIR spectrum changes considerably with the appearance of new absorptions associated with significant oxidation of the BP lattice after ambient exposure. Figure 4 shows the appearance of symmetric P-O-P vibrations at 850 cm^{-1} and asymmetric P-O-P stretches[33,36] at 710 and 770 cm^{-1}, indicating the formation of bridging oxide species, which is in excellent agreement with the O 1s core level. Additionally, a reduction in the O=P-OH peak intensity at 1650 cm^{-1} further supports conversion of non-bridging P-O species to bridging oxide species. The broadening of the P=O absorption and shift to 1430 cm^{-1} often occur as a result of the incorporation of hydrogen bonding[37] due to physisorption prior to chemical reaction with ambient water. An increase in the intensity of asymmetric PO_2 stretches at 1270 cm^{-1} and appearance of symmetric PO_2 stretches[36] at 1190

cm^{-1} also occur as BP oxidizes. Furthermore, the PO$_3$ stretches shift to 993 cm^{-1} and 1170 cm^{-1} which can be attributed to protonation of P-O species[32,38] to form P-OH groups. Bridging oxide species are highly reactive and readily react under ambient conditions as demonstrated by the reaction of phosphorus pentoxide which forms phosphoric acid after ambient exposure.[17] Protonation of P-O species suggests ambient water interacts with BP surface oxides to produce phosphoric acid. The shift and increase in intensity of PO$_3$ absorptions to form P-OH groups and a reduction in P=O peak intensity, as shown in Figure 4, also support the conversion of P=O groups to H$_3$PO$_4$ through reaction with water. This experimental observation is also in agreement with DFT studies.[25] Additionally, XPS analysis of the final product of degradation is displayed in Figure S4 (see Supporting Information) with a peak at 134.3 eV corresponding to the BE of phosphoric acid.[18] Initial formation of phosphoric acid cannot be deconvoluted from the oxide shoulder and when present in low concentrations liquid oxidation products may be removed under the vacuum of the XPS instrument.[17,18] After 3 days of ambient exposure the intensity of the PO$_2$ and the P-O-P absorption peaks increase as a result of further oxidation of BP. However, after a 1 week period in ambient conditions a large decrease is observed in all signals associated with phosphorus oxides. The reduction of all P-O peaks and protonated PO$_3$ absorptions is consistent with evaporation of volatile oxide species such as phosphoric acid from the surface of BP.

The presence of absorption peaks associated with O=P-OH and P-O species and the absence of P-O-P species both indicate that freshly exfoliated BP is characterized by the presence of primarily non-bridging oxide species, which is in excellent agreement with XPS analysis of the O 1s core level. Therefore, the BP lattice oxidizes through the formation of bridging P-O-P species which are highly unstable and susceptible to hydrolysis.[28] The reduction of the P-O-P component observed in XPS and absorptions observed in ATR-FTIR analysis indicate

conversion of bridging oxide species to phosphoric acid which suggests an oxidation cycle occurs. This continuous cycle results in the removal of the surface layers from the BP surface.[11,14,17,18] Literature reports vary in their discussion of the effect of water on the degradation of BP, but when combined with oxygen and light, water often facilitates oxidation.[15] Theoretical studies predict a hydrophobic BP surface that interacts more favorably with oxygen rather than water.[25] Therefore, the initial oxidation is most likely a result of the reaction of oxygen with the BP surface.[23] Theoretical calculations have shown that oxidized few-layer BP reacts exothermically with water[25] in agreement with our results where surface oxides react to form phosphoric acid through interaction with ambient water, which is also in correlation with studies on mechanically exfoliated few-layer BP by Favron *et. al.*[21] A key difference in our study is the use of liquid exfoliated BP rather than mechanically exfoliated BP which displays a shorter lifetime in ambient conditions. Solvent passivation has been reported to contribute to a higher stability in solution for liquid exfoliated BP in N-cyclohexyl-2-pyrrolidone, where a solvation shell protects flakes from oxidation.[4] The N 1s:P 2p ratios are displayed in Figure S5 and can be used as an indication of the amount of solvent passivating the surface after removal from solution. The N 1s:P 2p ratio for freshly exfoliated BP at 0.38 decreases to 0.18 after 1 week which further decreases to 0.13 after 2 weeks of ambient exposure. Comparison of the N 1s:P 2p ratio to the percentage of oxide determined from the P 2p core level shows a more significant increase in the oxide as the solvent is removed (Figure S5). The increased stability of solvent passivated flakes is in correlation with experimental studies by Abellán *et. al.*[13] where NMP-passivated BP displays a longer lifetime compared to THF-passivated or pristine BP. Therefore, solvent passivation also contributes to the stability of BP when flakes are removed from solution.
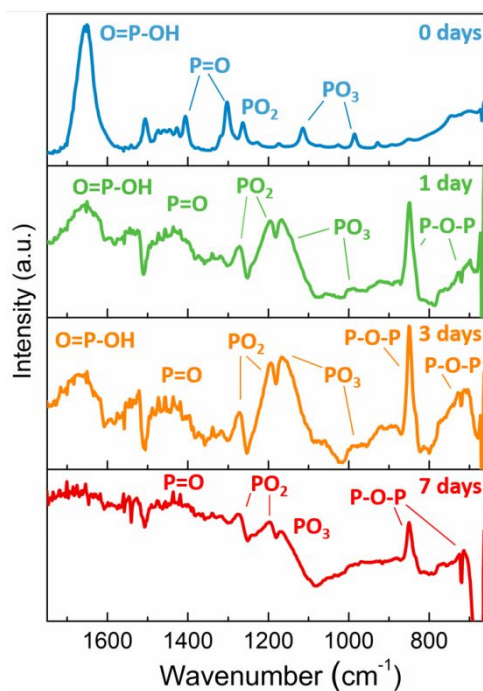
Figure 4: ATR-FTIR analysis of degrading BP exposed to ambient conditions over a 1 week period

Table 1: IR frequencies of few-layer BP over a period of 0 days to 1 week.

IR Frequencies of Black Phosphorus Surface Species				
Phosphorus Group	**0 days (cm⁻¹)**	**1 day (cm⁻¹)**	**3 days (cm⁻¹)**	**7 days (cm⁻¹)**
O=P-OH	1655	1655	1665	-
P=O	1406	1430	1450	-
P=O	1302	-	-	-
$(PO_2)_s$	-	1196	1194	1197
$(PO_2)_{as}$	1263	1272	1272	1272
$(PO_3)_s$	1115	1165	1163	1165
$(PO_3)_{as}$	985	995	992	-

14

$(P-O-P)_s$	-	850	850	850
$(P-O-P)_{as}$	-	770, 700	773, 706	770, 710

The stability of few-layer BP was monitored by STEM (Figure 5 and Figure S6 in Supporting Information), TEM (Figure S7 in Supporting Information) and AFM (Figure S8 in Supporting Information) to give a visual representation of BP degradation. Freshly exfoliated BP shown in Figure 5(a) displays flakes with well-defined edges. Surface protrusions due to BP oxidation can be seen clearly in Figure 5(b) and Figure S6-7 (see Supporting Information) for BP exposed to ambient conditions for 1 week. AFM analysis similarly shows loss of the BP structure with rounding flakes edges and formation of liquid droplets on the BP surface after ambient exposure as shown in Figures S8(a)-(b) (see Supporting Information). Multilayered bulk BP collected from the sediment of the first centrifuge cycle was used as a comparison to few-layer BP. The sediment was comprised of a mixture of flakes with varying thicknesses. Interestingly, multilayered bulk BP did not display the same oxidation pattern as few-layer BP at the edges. Surface protrusions similar to those on few-layer BP, were also observed on the multilayered bulk BP surface but the crystal edges remained well-defined after 1 week of ambient exposure, as displayed in Figure S8(c) (see Supporting Information). AFM and STEM analysis both corroborate the formation of liquid oxides, e.g. phosphoric acid, due to the appearance of liquid droplets on few-layer BP flakes rather than the formation of a stable oxide, demonstrating a key difference in oxidation behavior between few-layer and multilayered bulk BP.
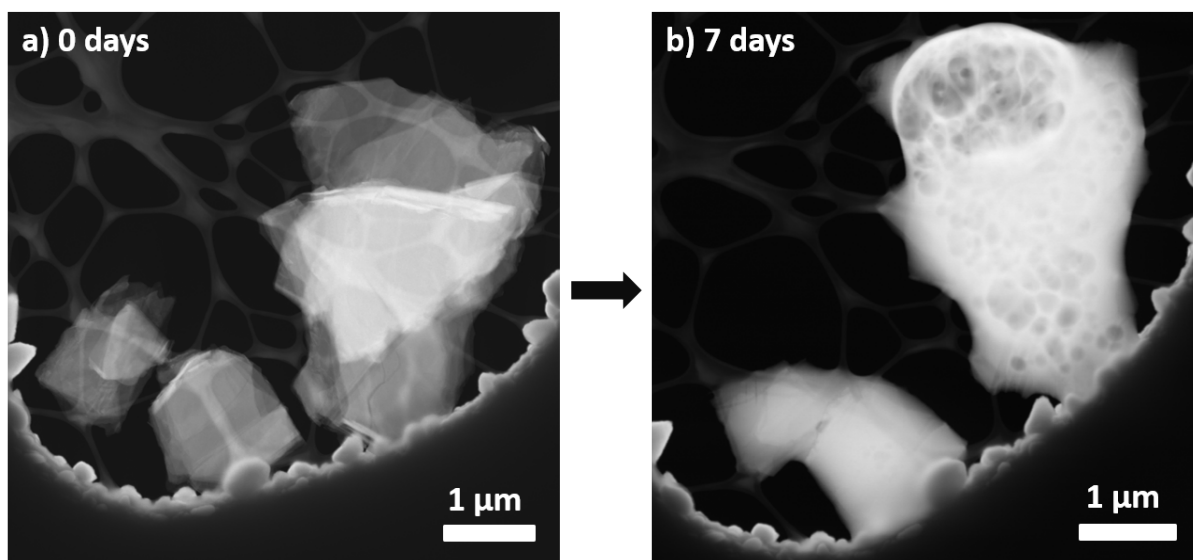
Figure 5: STEM analysis of (a) freshly exfoliated BP and (b)-(c) after 1 week air exposure.

The different degradation chemistries can also be observed by comparison of the O 1s and P 2p peaks after ambient exposure. Figure 6 displays the P 2p core level of bulk BP after 1 week of ambient exposure showing the oxide component increases from 20.3 % to 40.1 %. The O 1s displayed in Figure S9 (see Supporting Information) did not show the formation of a P-O-P component as in the case of few-layer BP, suggesting the formation of a surface oxide but no major oxidation of the BP lattice structure. In comparison, few-layer flakes only displayed an increase of 6 % in the P 2p oxide shoulder, as seen in Figures 2(a)-(c), and additionally oxidation occurred through the formation of volatile oxidation products which were removed under vacuum conditions. The difference in degradation chemistry of few-layer flakes stems from the formation of P-O-P species which facilitates more significant degradation. The absence of P-O-P formation for multilayered bulk BP allows the preservation of the crystal structure while the formation of a surface oxide is in correlation with experimental studies by Edmonds *et. al.*[18]. Higher reactivity for decreasing layer thickness was also observed by Favron *et. al.*[21] which was attributed to greater overlap between the band edge as a result of the

shift in band gap for lower flake thicknesses. Therefore, few-layer BP shows much more significant oxidation due to the formation of P-O-P species while multilayered bulk BP displays minor oxidation, in correlation with the formation of a surface oxide.
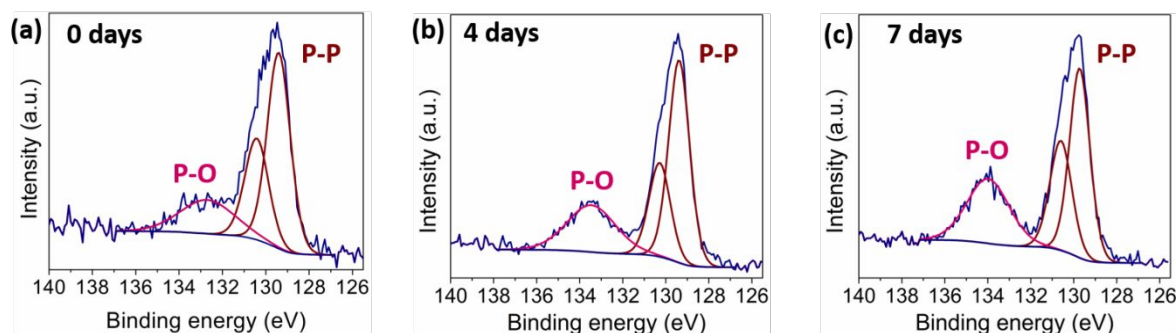
Figure 6: P 2p core levels displaying the oxidation of bulk BP over the period of 7 days.

Conclusions

We have investigated the degradation chemistry of liquid exfoliated few-layer BP exposed to ambient conditions using XPS and ATR-FTIR spectroscopy. Oxidation of BP initially occurs through the formation of non-bridging oxide species which convert to bridging oxide species (P-O-P) within 48 h of ambient exposure. The appearance of P-O-P species was monitored through XPS and ATR-FTIR analysis showing further oxidation leads to the conversion of bridging oxide species to phosphoric acid which subsequently evaporates from the BP surface. We also demonstrate the differences in degradation behavior between multilayered bulk and few-layer BP with multilayered bulk BP displaying higher stability due to the absence of bridging oxide species formation during ambient exposure. The successful determination of the degradation chemistry can assist in the discovery of targeted protection methods of BP.

Supporting Information.

Additional characterization of BP including STEM, TEM, XPS spectra and AFM analysis.

References

(1)   Liu, H., Neal, A. T., Zhu, Z., Luo, Z., Xu, X., Tománek, D., & Peide, D. Y.

        Phosphorene : An Unexplored 2D Semiconductor with a High Hole Mobility. *ACS

        Nano* **2014**, *8* (4), 4033–4041.

(2)   Li, L.; Yu, Y.; Ye, G. J.; Ge, Q.; Ou, X.; Wu, H.; Feng, D.; Chen, X. H.; Zhang, Y.

        Black Phosphorus Field-Effect Transistors. *Nat. Nanotechnol.* **2014**, *9* (5), 372–377.

(3)   Koenig, S. P.; Doganov, R. A.; Schmidt, H.; Castro Neto, A. H.; Özyilmaz, B. Electric

        Field Effect in Ultrathin Black Phosphorus. *Appl. Phys. Lett.* **2014**, *104* (10), 103-106.

(4)   Hanlon, D.; Backes, C.; Doherty, E.; Cucinotta, C. S.; Berner, N. C.; Boland, C.; Lee,

        K.; Harvey, A.; Lynch, P.; Gholamvand, Z.; et. al. Liquid Exfoliation of Solvent-

        Stabilized Few-Layer Black Phosphorus for Applications beyond Electronics. *Nat.

        Commun.* **2015**, *6*, 8563.

(5)   Zhang, Y.; Zheng, Y.; Rui, K.; Hng, H. H.; Hippalgaonkar, K.; Xu, J.; Sun, W.; Zhu,

J.; Yan, Q.; Huang, W. 2D Black Phosphorus for Energy Storage and Thermoelectric Applications. *Small* **2017**, *13* (28), 1–20.

(6)   Gusmao, R.; Sofer, Z.; Pumera, M. Black Phosphorus Rediscovered: From Bulk to Monolayer. *Angew. Chemie Int. Ed.* **2017**, *56* (28), 8052–8072.

(7)   Huang, S.; Ling, X. Black Phosphorus: Optical Characterization, Properties and Applications. *Small* **2017**, *13* (38), 1–18.

(8)   Xue, Y.; Zhang, Q.; Zhang, T.; Fu, L. Black Phosphorus: Properties, Synthesis, and Applications in Energy Conversion and Storage. *ChemNanoMat* **2017**, *3* (6), 352–361.

(9)   Rodin, A. S.; Carvalho, A.; Castro Neto, A. H. Strain-Induced Gap Modification in Black Phosphorus. *Phys. Rev. Lett.* **2014**, *112* (17), 1–5.

(10)   Ziletti, A.; Carvalho, A.; Campbell, D. K.; Coker, D. F.; Castro Neto, A. H. Oxygen Defects in Phosphorene. *Phys. Rev. Lett.* **2015**, *114* (4), 26–29.

(11)   Castellanos-Gomez, A.; Vicarelli, L.; Prada, E.; Island, J. O.; Narasimha-Acharya, K. L.; Blanter, S. I.; Groenendijk, D. J.; Buscema, M.; Steele, G. a.; Alvarez, J. V.; et. al. Isolation and Characterization of Few-Layer Black Phosphorus. *2D Mater.* **2014**, *1* (2), 025001.

(12)   Wood, J. D.; Wells, S. A.; Jariwala, D.; Chen, K. S.; Cho, E.; Sangwan, V. K.; Liu, X.; Lauhon, L. J.; Marks, T. J.; Hersam, M. C. Effective Passivation of Exfoliated Black Phosphorus Transistors against Ambient Degradation. *Nano Lett.* **2014**, *14* (12), 6964–6970.

(13)   Abellán, G.; Wild, S.; Lloret, V.; Scheuschner, N.; Gillen, R.; Mundloch, U.; Maultzsch, J.; Varela, M.; Hauke, F.; Hirsch, A. Fundamental Insights into the Degradation and Stabilization of Thin Layer Black Phosphorus. *J. Am. Chem. Soc.*
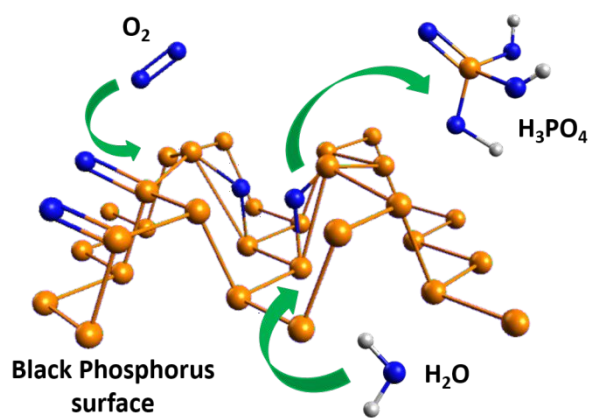
2017, *139* (30), 10432–10440.

(14)   Island, J. O.; Steele, G. A.; Zant, H. S. J. van der; Castellanos-Gomez, A. Environmental Instability of Few-Layer Black Phosphorus. *2D Mater.* **2015**, *2* (1), 011002.

(15)   Hu, Z.; Li, Q.; Lei, B.; Zhou, Q.; Xiang, D.; Lyu, Z.; Hu, F.; Wang, J.; Ren, Y.; Guo, R.; et. al. Water-Catalyzed Oxidation of Few-Layer Black Phosphorous in a Dark Environment. *Angew. Chemie - Int. Ed.* **2017**, *56* (31), 9131–9135.

(16)   Yang, T.; Dong, B.; Wang, J.; Zhang, Z.; Guan, J.; Kuntz, K.; Warren, S. C.; Tománek, D. Interpreting Core-Level Spectra of Oxidizing Phosphorene: Theory and Experiment. *Phys. Rev. B - Condens. Matter Mater. Phys.* **2015**, *92* (12), 125412.

(17)   Kuntz, K. L.; Wells, R. A.; Hu, J.; Yang, T.; Dong, B.; Guo, H.; Woomer, A. H.; Druffel, D. L.; Alabanza, A.; Tománek, D.; et. al. Control of Surface and Edge Oxidation on Phosphorene. *ACS Appl. Mater. Interfaces* **2017**, *9* (10), 9126–9135.

(18)   Edmonds, M. T.; Tadich, A.; Carvalho, A.; Ziletti, A.; O'Donnell, K. M.; Koenig, S. P.; Coker, D. F.; Özyilmaz, B.; Neto, A. H. C.; Fuhrer, M. S. Creating a Stable Oxide at the Surface of Black Phosphorus. *ACS Appl. Mater. Interfaces* **2015**, *7* (27), 14557–14562.

(19)   Luo, W.; Zemlyanov, D. Y.; Milligan, C. A.; Du, Y.; Yang, L.; Wu, Y.; Ye, P. D. Surface Chemistry of Black Phosphorus under a Controlled Oxidative Environment. *Nanotechnology* **2016**, *27* (43), 434002.

(20)   Wang, G.; Slough, W. J.; Pandey, R.; Karna, S. P. Degradation of Phosphorene in Air: Understanding at Atomic Level. *2D Mater.* **2016**, *3* (2), 025011.

(21)   Favron, A.; Gaufrès, E.; Fossard, F.; Phaneuf-L'Heureux, A.-L.; Tang, N. Y.-W.;

Lévesque, P. L.; Loiseau, A.; Leonelli, R.; Francoeur, S.; Martel, R. Photooxidation and Quantum Confinement Effects in Exfoliated Black Phosphorus. *Nat. Mater.* **2015**, *14* (8), 826–832.

(22)   Woomer, A. H.; Farnsworth, T. W.; Hu, J.; Wells, R. A.; Donley, C. L.; Warren, S. C. Phosphorene: Synthesis, Scale-Up, and Quantitative Optical Spectroscopy. *ACS Nano* **2015**, *9* (9), 8869–8884.

(23)   Huang, Y.; Qiao, J.; He, K.; Bliznakov, S.; Sutter, E.; Chen, X.; Luo, D.; Meng, F.; Su, D.; Decker, J.; et. al. Interaction of Black Phosphorus with Oxygen and Water. *Chem. Mater.* **2016**, *28* (22), 8330–8339.

(24)   Chen, L.; Zhou, G.; Liu, Z.; Ma, X.; Chen, J.; Zhang, Z.; Ma, X.; Li, F.; Cheng, H. M.; Ren, W. Scalable Clean Exfoliation of High-Quality Few-Layer Black Phosphorus for a Flexible Lithium Ion Battery. *Adv. Mater.* **2016**, *28* (3), 510–517.

(25)   Wang, G.; Slough, W. J.; Pandey, R.; Karna, S. P. Degradation of Phosphorene in Air: Understanding at Atomic Level. *2D Mater.* **2016**, *3* (2), 025011.

(26)   Xu, W. P.; Xu, H. Role of Surface Adsorption in Tuning the Properties of Black Phosphorus. *Phys. Chem. Chem. Phys.* **2017**, 112–117.

(27)   Zhou, Q.; Chen, Q.; Tong, Y.; Wang, J. Light-Induced Ambient Degradation of Few-Layer Black Phosphorus: Mechanism and Protection. *Angew. Chemie - Int. Ed.* **2016**, *55* (38), 11437–11441.

(28)   Ewig, C. S.; Van Wazer, J. R. Ab Initio Structures of Phosphorus Acids and Esters. 3. The P-O-P Bridged Compounds H4P2O2n-1 for n = 1 to 4. *J. Am. Chem. Soc.* **1988**, *110* (1), 79–86.

(29)   Liu, H.; Du, Y.; Deng, Y.; Ye, P. D. Semiconducting Black Phosphorus: Synthesis,

Transport Properties and Electronic Applications. *Chem. Soc. Rev* **2732**, *44* (44), 2732–2743.

(30)   Wang, Y.; Sherwood, P. M. A. Phosphorus Pentoxide (P2O5) by XPS. *Surf. Sci. Spectra* **2002**, *9* (1), 159.

(31)   Colthup, N. *Introduction to Infrared and Raman Spectroscopy*; Elsevier, 2012.

(32)   Gong, W. A Real Time in Situ ATR-FTIR Spectroscopic Study of Linear Phosphate Adsorption on Titania Surfaces. *Int. J. Miner. Process.* **2001**, *63* (3), 147–165.

(33)   Omrani, R. O.; Krimi, S.; Videau, J. J.; Khattech, I.; El Jazouli, A.; Jemal, M. Structural and Thermochemical Study of Na2O–ZnO–P2O5 Glasses. *J. Non. Cryst. Solids* **2014**, *390*, 5–12.

(34)   Nogami, M. Proton Conductivity in Sol–gel-Derived P2O5–TiO2–SiO2 Glasses. *Solid State Ionics* **2004**, *166* (1–2), 39–43.

(35)   Ahsan, M. R.; Uddin, M. A.; Mortuza, M. G. Infrared Study of the Effect of P 2O5 in the Structure of Lead Silicate Glasses. *Indian J. pure Appl. Phys.* **2005**, *43* (February), 89–99.

(36)   Chahine, A.; Et-tabirou, M. Structural Study of (50-x)Na2O-CuO-10Bi2O3-40P2O5 Glasses. **2002**, *37*, 1973–1979.

(37)   Paniagua, S. a; Hotchkiss, P. J.; Jones, S. C.; Marder, S. R.; Mudalige, A.; Marrikar, F. S.; Pemberton, J. E.; Armstrong, N. R. Phosphonic Acid Modification of ITO Electrodes - Combined XPS - UPS - Contact Angle Studies. *J. Phys. Chem. C* **2008**, *112* (21), 7809–7817.

(38)   Robinson, E. a. Characteristic Vibrational Frequencies of Oxygen Compounds of Silicon, Phosphorus, and Chlorine: Correlation of Stretching Frequencies and Force

Constants With Bond Lengths and Bond Orders. *Can. J. Chem.* **1963**, *41* (12), 3021–3033.

TOC Figure